

## Metallic Normal State of $Y_1Ba_2Cu_3O_{7-\delta}$

Milind N. Kunchur,<sup>1,\*</sup> B. I. Ivlev,<sup>2</sup> D. K. Christen,<sup>3</sup> and J. M. Phillips<sup>4</sup>

<sup>1</sup>*Department of Physics and Astronomy, University of South Carolina, Columbia, South Carolina 29208*

<sup>2</sup>*Instituto de Física, Universidad Autónoma de San Luis Potosí, San Luis Potosí, Mexico*

<sup>3</sup>*Solid State Division, Oak Ridge National Laboratory, Oak Ridge, Tennessee 37831*

<sup>4</sup>*Sandia National Laboratory, M/S 1411, Albuquerque, New Mexico 87185-1411*

(Received 30 November 1999)

Flux flow was studied over an entire temperature range down to  $T \sim 2\%$  of  $T_c$  by using intense pulsed current densities to overcome flux-vortex pinning. The resistivity at high vortex velocities is proportional to  $B$  and roughly follows  $\rho \sim \rho_n B/H_{c2}$ , with a prefactor of order unity. Contrary to some speculation,  $\rho_n$  saturates to a finite residual value as  $T \rightarrow 0$ , indicating a metallic ( $\rho \rightarrow \text{finite}$ ) rather than insulating ( $\rho \rightarrow \infty$ ) normal state, and the vortex dissipation continues to be conventional as  $T \rightarrow 0$ .

PACS numbers: 74.40.+k, 74.60.Ge, 74.72.Bk

An important property of any superconductor is the behavior of the normal state both above and below  $T_c$ . The traditional way to probe the normal-state resistivity  $\rho_n$  below  $T_c$  is to apply a magnetic field  $H$  greater than the upper critical value  $H_{c2}$ . In high-temperature superconductors, however,  $\rho_n$  for  $T \rightarrow 0$  continues to be an elusive quantity because  $H_{c2} \sim 100$  T. Such fields can introduce substantial magnetoresistance and potentially induce a transformation between metallic and insulating states. Indeed the present controversy in some systems is not over the precise value of  $\rho_n$  ( $T \rightarrow 0$ ), but whether it is infinite [1] or finite [2]. One alternative to applying large fields  $H > H_{c2}$  is to prepare samples with different compositions and doping to study how  $\rho_n$  varies as  $T_c$  is suppressed. While avoiding the problem of magnetoresistance, this method introduces changes in other parameters such as carrier concentration.

In this paper we use a third tool to probe  $\rho_n$  below  $T_c$ , which is the flow of magnetic flux vortices. The effective resistivity of the core that governs vortex dissipation is in many cases closely tied to  $\rho_n$ . Even when deviations arise in special cases, the measurement can still allow differentiation between insulating ( $\rho \rightarrow \infty$ ) and metallic ( $\rho \rightarrow \text{finite}$ ) behaviors. Because the flux-flow method uses low flux densities ( $B \ll H_{c2}$ ) only to introduce vortices and the composition of the original system is unaltered, it provides a valuable complement to the other two approaches in helping to build a picture of the elusive normal state below  $T_c$ .

At fields greater than the lower critical value  $H_{c1}$ , a type-II superconductor contains flux vortices each carrying a quantum of flux  $\Phi_0 = h/2e$  Wb. A transport current density  $j$  exerts a Lorentz driving force  $\mathbf{j} \times \Phi_0$  on the vortices, with the motion being opposed by a viscous drag  $\eta v$  ( $\eta$  is the coefficient of viscosity), so that in steady state  $j\Phi_0 = \eta v$  and the response is Ohmic. Larkin and Ovchinnikov have shown that a dirty superconductor at low temperatures has a flux-flow resistivity given

by [3]

$$\rho_f/\rho_n \approx 0.9B/H_{c2}(T). \quad (1)$$

Approximately the same result, without the precise 0.9 prefactor, can be obtained by considering the Ohmic dissipation in the core and temporal changes in the order parameter leading to irreversible entropy transfer [4]; the result is also valid for  $d$ -wave superconductors that are not superclean [5]. Equation (1) is equivalent to  $\eta \approx \Phi_0 H_{c2}/\rho_n$  and  $\eta \propto \Delta$ , the superconducting order parameter.

At low values of  $j$ , the response is non-Ohmic due to pinning, and the purely viscous free-flux-flow (FFF) regime is accessed when  $j \gg j_c$ , where  $j_c$  is the depinning threshold (e.g., see Fig. 5 of Ref. [6]). Our previous work [7] close to  $T_c$  ( $T_c > T > 0.85T_c$ ) confirmed this behavior [8]. As shown in Fig. 1(a), at sufficiently large  $j$ ,  $\rho(j)$  shows a tendency to saturate to a constant value with a resistivity in agreement with Eq. (1).

At low temperatures, larger current densities and vortex velocities  $v_\phi$  are required to fully overcome pinning and promote free-flux flow. Such conditions may induce changes in the electronic distribution function and the structure of the vortex [9], causing a non-Ohmic response and deviations from Eq. (1). Under conditions of extremely high  $j$  and  $v_\phi$ , the viscosity may drop so rapidly with  $v_\phi$  that the vortex motion becomes unstable, causing a discontinuous jump in  $E$  above a threshold  $j^*$ . Figures 1(b) and 1(c) show resistivity curves at two lower temperatures, 50 and 20 K, up to this instability. As expected from the above discussion, there is some deviation from Ohmic behavior and the measured resistivities continue to climb with  $j$  after pinning is overcome. From the data it appears that the increase over  $\rho_f$  is by a factor of order unity. Note that this correction affects only the exact value of  $\rho_n$  that is extracted, not the conclusion of whether the normal state is metallic or insulating. Previous theoretical work on the vortex instability, which has concentrated on

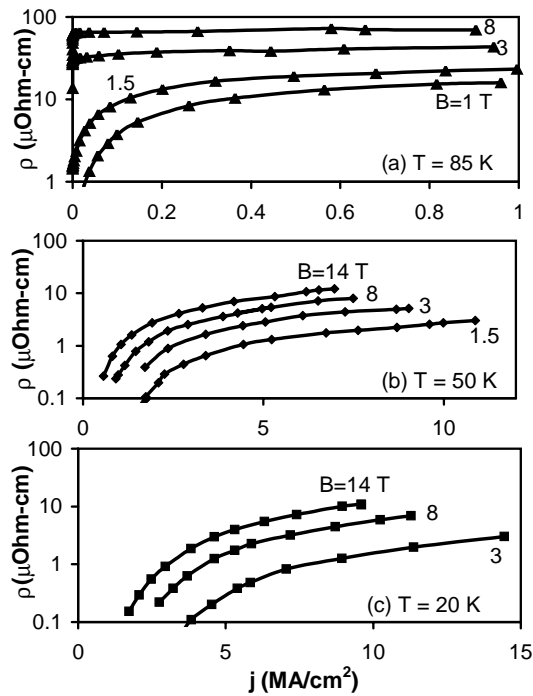


FIG. 1. (a)  $\rho$ - $j$  curves from Ref. [7] showing saturation into FFF behavior at high  $T$ . (b), (c)  $\rho$ - $j$  curves at lower temperatures (sample L2) showing some nonlinearity.

the region near  $T_c$  [9], finds the critical resistivity at instability  $\rho^*$  to be proportional to  $\rho_f$ . For low  $T$  we estimate below that  $\rho^* \sim 2\rho_f$ .

For  $T \ll T_c$  most of the carriers are condensed: A main manifestation of the nonequilibrium energy rise is to break pairs and create quasiparticles. For our conditions, the energy-relaxation length ( $l_\epsilon = \sqrt{D\tau_\epsilon} \sim 100$ – $1000$  nm) is larger than the intervortex spacing ( $l_\phi = 1.075\sqrt{\Phi_0/B} \sim 10$ – $50$  nm) and a comparison of scattering rates (extrapolated to low temperatures) indicates that electron-electron scattering is likely to be more rapid than electron-phonon scattering; here  $D = 3 \times 10^{-4}$  m<sup>2</sup>/s is the diffusion constant and  $\tau_\epsilon \sim 0.1$ – $10$  ns is the energy-relaxation (electron-phonon) time. The nonequilibrium shift in the energy density of the electronic system is  $jE\tau_\epsilon$ . If  $\delta n_n$  is the number of quasiparticles created, we have  $\Delta\delta n_n \approx jE\tau_\epsilon$ . Since  $\Delta^2 \propto n_s = n - n_n$  (where  $n$  is the carrier concentration and  $n_s$  is half the pair density) and  $\eta \propto \Delta$ , the dissipation-dependent viscosity becomes  $\eta(E) = \eta(0)(1 - jE\tau_\epsilon/2n\Delta)$ . Making use of  $E = v_\phi B$ ,  $\eta v_\phi = j\Phi_0$ , and  $\eta(0) \approx \Phi_0 H_{c2}/\rho_n$ , we find  $j\rho_f \sim E/[1 + (E/E^*)^2]$  with  $E^* = \sqrt{2\rho_f n \Delta/\tau_\epsilon}$ . The instability occurs at  $E = E^*$ , where  $j$  reaches its maximum value  $j^*$ . Here

$$\rho^* \equiv E^*/j^* \approx 2\rho_f \approx 2\rho_n B/H_{c2}. \quad (2)$$

This supports what was earlier deduced empirically from the data of Fig. 1, that  $\rho^*$  is only slightly higher (within an order of unity) than  $\rho_f$  upon reaching the instability. [Additional corrections to Eqs. (1) and (2) can occur in an

$s$ -wave superconductor with very short coherence length  $\xi$ , where the large core-level spacing can make vortex dissipation vanish as  $T \rightarrow 0$ . A related consequence has been seen in the Nernst effect in  $\text{Nd}_{1.85}\text{Ce}_{0.15}\text{CuO}_{4-\delta}$  [10]. However,  $\text{Y}_1\text{Ba}_2\text{Cu}_3\text{O}_{7-\delta}$  does not satisfy  $2\xi \ll l$ , with a mean-free path  $l \sim 5$  nm and  $\xi(T) \sim 1.6$  nm, and gap nodes allow quasiparticles to extend out even farther. This is consistent with our observed finite vortex dissipation as  $T \rightarrow 0$ . For the same reasons the Kramer-Pesch effect [11], which applies to ultraclean  $s$ -wave superconductors, is not relevant for  $\text{Y}_1\text{Ba}_2\text{Cu}_3\text{O}_{7-\delta}$ .]

The samples are 90-nm-thick  $c$ -axis oriented epitaxial films of  $\text{Y}_1\text{Ba}_2\text{Cu}_3\text{O}_{7-\delta}$  on a (100)  $\text{LaAlO}_3$  substrate. The films were prepared using the  $\text{BaF}_2$  process, described elsewhere [12], with conditions optimized to produce single-crystal like quality [7]. Electron-beam and optical-projection lithographies, together with wet etching in  $\sim 1\%$  phosphoric acid, were used for patterning. This study includes two small ( $\approx 3 \times 50 \mu\text{m}^2$ ), two medium ( $8 \times 100 \mu\text{m}^2$ ), and two large ( $16 \times 180 \mu\text{m}^2$ ) bridges, labeled S1, S2, M1, M2, L1, and L2. Figure 1 also includes for comparison data from our earlier Letter [7] for a  $100 \times 3000 \mu\text{m}^2$  bridge. The zero-resistance  $T_c$ 's are about 90 K with transition widths  $\sim 0.5$  K.

The results are very reproducible and independent of sample size. The inset of Fig. 2 compares the resistive transitions of a small (S1) and a medium (M1) bridge. The main panel of Fig. 2 shows mixed-state  $j$ - $\rho$  curves for samples of three different widths. In the superconducting state a transport current is liable to travel along the edges of a bridge, making it difficult to define a bulk resistivity [13]. However, at higher dissipations, current flow should become uniform because of the principle of minimum entropy production. This is born out by Fig. 2, where the curves for all widths converge at high  $j$ .

The flux densities used in this paper (0.7–16 T, with  $B \perp \text{CuO}$  planes) exceed the self-field of the current by

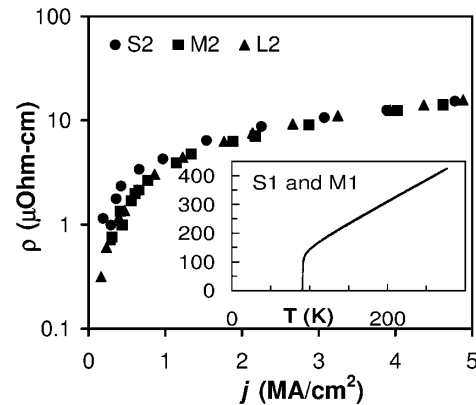


FIG. 2. Mixed-state characteristics at three sample widths (S2 is 2.8, M2 is 8, and L2 is 16  $\mu\text{m}$ ) at  $T = 50$  K,  $B = 13.8$  T.  $\rho(j)$  becomes universal at large  $j$ , verifying current-flow uniformity. The inset shows closely overlapping resistive transitions of samples S1 (3  $\mu\text{m}$  wide) and M1 (8  $\mu\text{m}$  wide).

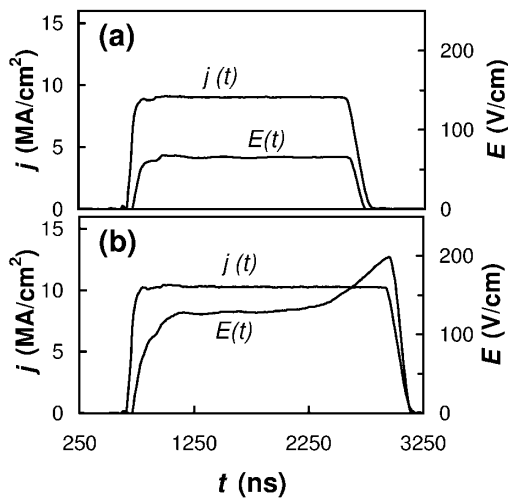


FIG. 3. Oscilloscope traces for sample S1 at  $T = 25$  K and  $B = 13.8$  T. (a) Subcritical values of  $E$  and  $j$ . (b) Temporal development of the vortex instability as  $j$  exceeds the critical threshold.

at least 2 orders of magnitude. In the region of interest the current density satisfies  $j_c \ll j \ll j_0$  (with  $j \parallel$  CuO planes) minimizing the influence of pinning; here  $j_0 \sim 10^8$  A/cm<sup>2</sup> is the depairing current density [14]. These conditions provide a homogeneous system ideal for studying intrinsic vortex dissipation.

The electrical transport measurements are made with a pulsed current source, preamplifier, and digital oscilloscope. The measurement setup is discussed in a previous review article [15]. Figure 3 shows oscilloscope waveforms of current and voltage pulses just below (a) and above (b) the instability threshold. The pulse rise times are about 100 ns. The short rise times combined with narrow bridge widths permit transport measurements at dissipation densities in the  $10^9$  W/cm<sup>3</sup> range. We previously discussed [7,15] that the onset of bulk heating is signaled by a distortion in the voltage pulse, where  $E(t)$  becomes slanted beginning at  $t = 0$ . In the case of a vortex instability,  $E(t)$  is flat at short times and has an abrupt hump, as seen in Fig. 3(b). This hump expands dramatically with the slightest further increase of  $j$ . The aforementioned review article discusses our detailed procedures to rule out sample heating, involving empirical calibrations as well as first-principles calculations of the thermal resistance ( $R_{th} \sim 1$  nK cm<sup>3</sup>/W).

Figures 1(b) and 1(c) show some typical sets of  $j$ - $\rho$  curves for sample L2 at  $T = 50$  K and  $T = 20$  K at various fields.  $E$  varies smoothly with  $j$  until the last point where the appearance of a hump-shaped waveform distortion [Fig. 3(b)] coincides with a rapid divergence in  $E$ , which we identify as the point of vortex instability. The critical resistivities  $\rho^* = E^*/j^*$  (end points of the curves in Fig. 1) are plotted against  $B$  in Fig. 4. As predicted by Eq. (2), we see that  $\rho^*$  is proportional to  $B$  (intercept  $\rightarrow 0$  at large  $B$ ). Equation (2) now yields an

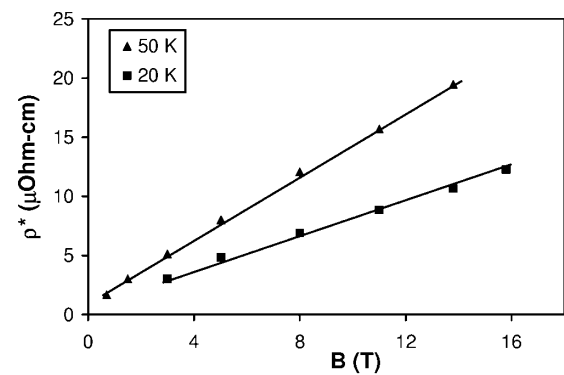


FIG. 4. Critical resistivities for sample L2 show homogeneous linearity at high flux densities.

estimate of  $\rho_n$  uncomplicated by the magnetoresistance of the normal state. The upper critical field  $H_{c2}$  and its complete temperature dependence are now well established [16,17], most recently using direct high fields (130 T) by Nakagawa *et al.* [16]. We use this empirical  $H_{c2}(T)$  [with  $H_{c2}(0) = 120$  T] to calculate  $\rho_n(T)$  from Eq. (2).

Figure 5 shows the final result, a picture of the approximate normal-state resistivity over the complete temperature range for sample M2. The high-temperature curve is the usual continuous current ( $j = 194$  A/cm<sup>2</sup>) measurement of the resistive transition. The dashed line at intermediate temperatures is a schematic representation of  $\rho_n$  deduced from our earlier work [7] on free-flux flow ( $0.85T < T < T_c$ ). The data below 60 K come from the critical resistivities measured in this paper. The overall temperature dependence is consistent with the measurement of  $\rho_n(T)$  in  $Y_1Ba_2Cu_3O_{7-\delta}$  by Nakagawa *et al.* [16] (allowing for a possibly large magnetoresistance) who suppressed the superconductivity by applying pulsed fields  $H > H_{c2}$ .

There are two key points about our results. First, this is a direct experimental confirmation, for  $Y_1Ba_2Cu_3O_{7-\delta}$ ,

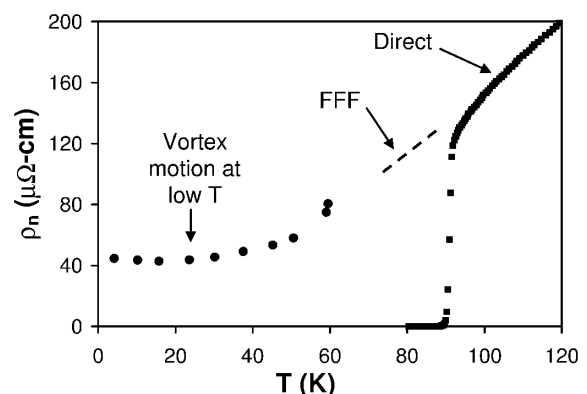


FIG. 5. The estimated normal-state resistivity over the entire temperature range. The squares are a direct measurement at  $j = 194$  A/cm<sup>2</sup>. The dashed line was deduced from free flux flow in earlier work [7]. The circles are the new data obtained in this work.

that the conventional ideas of vortex dissipation work all the way down to  $T \ll T_c$ , with a  $\rho_n$  of about the right value and a flow resistivity that is proportional to  $B$ . Second, in the controversy as to whether the normal state is insulating or metallic, the Boebinger *et al.* results [1] indicate the novel possibility of an insulating normal state. However, high fields near a metal-insulator transition (they use  $H > H_{c2} \sim 60$  T to quench superconductivity) can actually change the behavior from metallic to insulating [2]. Our flux-flow approach probes  $\rho_n$  at  $H \ll H_{c2}$ , and thus provides complementary information and further insight into the nature of the normal state in the zero-temperature limit.

The authors acknowledge technical assistance from J.E. Workman, J.W. Campbell, and the USC Electron Microscopy Center, and useful discussions with N.B. Kopnin, R.P. Huebener, J.M. Knight, C.P. Poole, P. Lindenfeld, V.G. Kogan, T.R. Lemberger, and A.A. Abrikosov. This work was supported by the U.S. Department of Energy through Grant No. DE-FG02-99ER45763.

---

\*<http://www.cosm.sc.edu/kunchur>

- [1] G.S. Boebinger *et al.*, Phys. Rev. Lett. **77**, 5417 (1996); Y. Ando *et al.*, Phys. Rev. Lett. **75**, 4662 (1995).
- [2] K. Karpińska *et al.*, Phys. Rev. Lett. **77**, 3033 (1996); A. Malinowski *et al.*, Phys. Rev. Lett. **79**, 495 (1997).
- [3] A.I. Larkin and Yu.N. Ovchinnikov, in *Nonequilibrium Superconductivity*, edited by D.N. Langenberg and A.I. Larkin (Elsevier, New York, 1986), Chap. 11, and references therein.
- [4] J. Bardeen and M.J. Stephen, Phys. Rev. **140**, A1197 (1965); M. Tinkham, Phys. Rev. Lett. **13**, 804 (1964); J.R. Clem, Phys. Rev. Lett. **20**, 735 (1968).
- [5] N.B. Kopnin and G.E. Volovik, Phys. Rev. Lett. **79**, 1377 (1997).
- [6] G. Blatter, M.V. Feigel'man, V.B. Geshkenbein, A.I. Larkin, and V.M. Vinokur, Rev. Mod. Phys. **66**, 1125 (1994).
- [7] M.N. Kunchur, D.K. Christen, and J.M. Phillips, Phys. Rev. Lett. **70**, 998 (1993).
- [8] Michael Tinkham, *Introduction to Superconductivity* (McGraw-Hill, New York, 1996), 2nd ed., p. 170.
- [9] A.I. Larkin and Yu.N. Ovchinnikov, Zh. Eksp. Teor. Fiz. **68**, 1915 (1975) [Sov. Phys. JETP **41**, 960 (1976)]; W. Klein, R.P. Huebener, S. Gauss, and J. Parisi, J. Low Temp. Phys. **61**, 413 (1985).
- [10] X. Jiang *et al.*, Physica (Amsterdam) **254C**, 175 (1995).
- [11] L. Kramer and W. Pesch, Z. Phys. **269**, 59 (1974); S.G. Doettinger *et al.*, Chin. J. Phys. **34**, 291 (1996).
- [12] M.P. Siegal *et al.*, J. Appl. Phys. **68**, 6353 (1990); D.J. Carlson *et al.*, J. Mater. Res. **5**, 2797 (1990).
- [13] E. Zeldov, J.R. Clem, M. McElfresh, and M. Darwin, Phys. Rev. B **49**, 9802 (1994).
- [14] M.N. Kunchur, D.K. Christen, C.E. Klabunde, and J.M. Phillips, Phys. Rev. Lett. **72**, 752 (1994).
- [15] M.N. Kunchur, Mod. Phys. Lett. B **9**, 399 (1995).
- [16] H. Nakagawa, N. Miura, and Y. Enomoto, J. Phys. Condens. Matter **10**, 11 571 (1998).
- [17] U. Welp *et al.*, Phys. Rev. Lett. **62**, 1908 (1989).